DANISH METEOROLOGICAL INSTITUTE

—— TECHNICAL REPORT ——

00-28

A sea ice forecasting system for the Cape Farewell area

Nicolai Kliem

ISSN 0906-897X (printed)
ISSN 1399-1388 (online)

DMI

Copenhagen 2000

A sea ice forecasting system for the Cape Farewell area

Nicolai Kliem

email: nk@dmi.dk
Danish Meteorological Institute

Contents

1 Introduction

A sea ice forecasting system is under development at the Danish Meteorological Institute (DMI). The objective is to predict sea ice drift in the waters around Cape Farewell 2-3 days in advance. The forecasts will be of benefit to the present ice service at DMI.

The Ice Charting and Remote Sensing Division at DMI produce maps of sea ice concentration in the Cape Farewell area. The maps are mainly used for safe navigation and are updated every 2-3 days. They are based on remotely sensed data, that is, satellite-borne measurements primarily from Radarsat, and by airborne measurements with a specially-equipped aircraft and helicopter. Development of the ice service at DMI goes in two directions. One is to exploit the number of different kinds of satellite observations [*Gill*, 1998; *Gill and Valeur*, 1999]. The other is to use numerical models to predict sea ice drift [*Kliem*, 1999], in order to produce forecasts of the ice extent a few days ahead and to fill the gap between two successive ice maps. This paper describes the forecasting system, and gives a validation of the pre-operational model performance for the 1999-2000 ice season.

2 Forecasting system

2.1 System description

The forecasting system is based on a numerical sea ice model and is intended to be an extension to the present ice service. The flowchart of sea ice prediction is shown in Fig. 1. When new observations are available, they are analyzed manually to produce a map of the sea ice concentration. This is the present ice service used for nowcasting, with the ice concentration map showing the current ice state. It is not considered as a part of the forecasting procedure, but as an independent system providing the necessary data for the initialization and validation of the forecasting system. The forecast procedure proceeds as follows. The analyzed ice concentration field is transformed to gridded data to be used as initial condition for the model. The analysed fields do not in general cover the entire model domain, and the missing initial values are filled by using the preceding forecast. The actual wind forecast and a climatological ocean state of currents are then forcing the ice drift model producing a forecast for the ice cover.

The philosophy behind the forcing is that the ocean (the East Greenland Current) gives a mean drag on the ice transporting it along the coast of Greenland, while the daily variations are mainly due to the wind. Thus, the actual wind forecast is essential for the ice drift forecasts on the short time scales, while it is sufficient with a realistic steady-state sea surface current field. In the simulations the wind drag thus tends to accelerate the ice, while the ocean drag tends to keep a steady motion.

Figure 2 illustrates the schedule of the forecasting system. Each time a new ice analysis is produced, this is used as initial condition for a new forecast. The observations do not necessary come in fixed interval, but the forecast period is long enough to cover the time span until the next available observations.

2.2 Sea ice model

The simulations of the ice drift is performed with a dynamic finite element sea ice model (described more detailed in Appendix 3). The model is based on a continuum formulation with a velocity, an ice thickness and an ice concentration field and the usual momentum and continuity

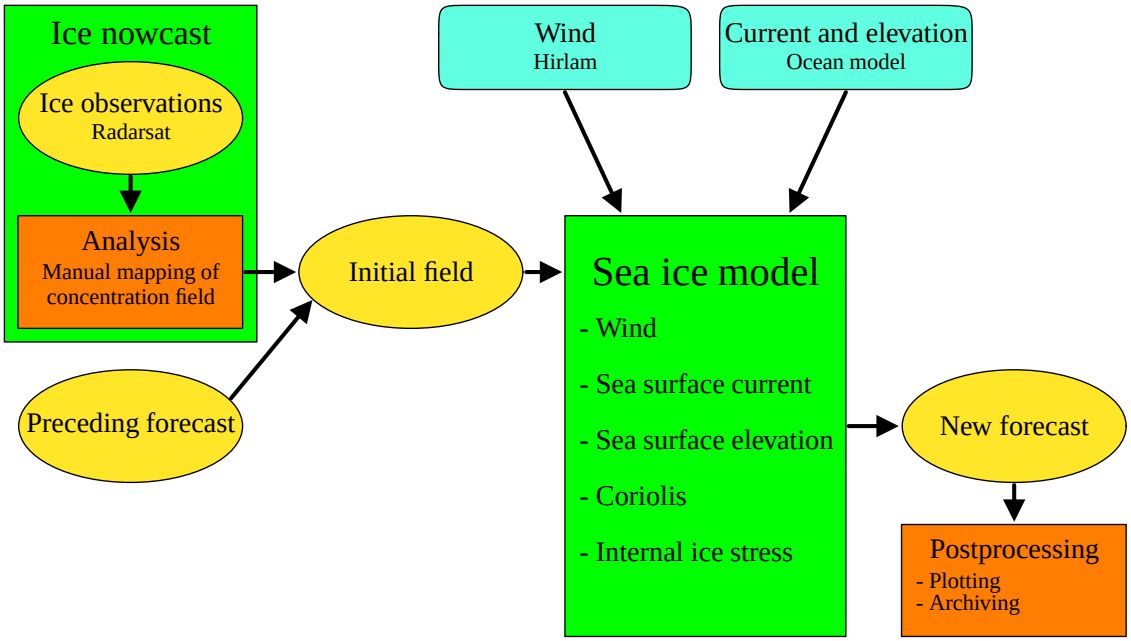

Figure 1. Sketch of the forecasting system. Initial ice concentration field is based on observations complemented by the preceding forecast. Forcing fields are read from an atmospheric forecasting model (Hirlam) and a diagnostic ocean model.

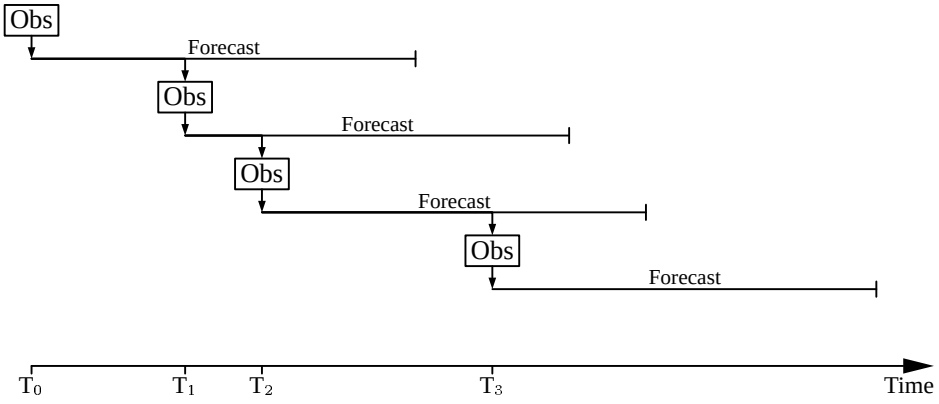

Figure 2. Schedule of the forecasting system.

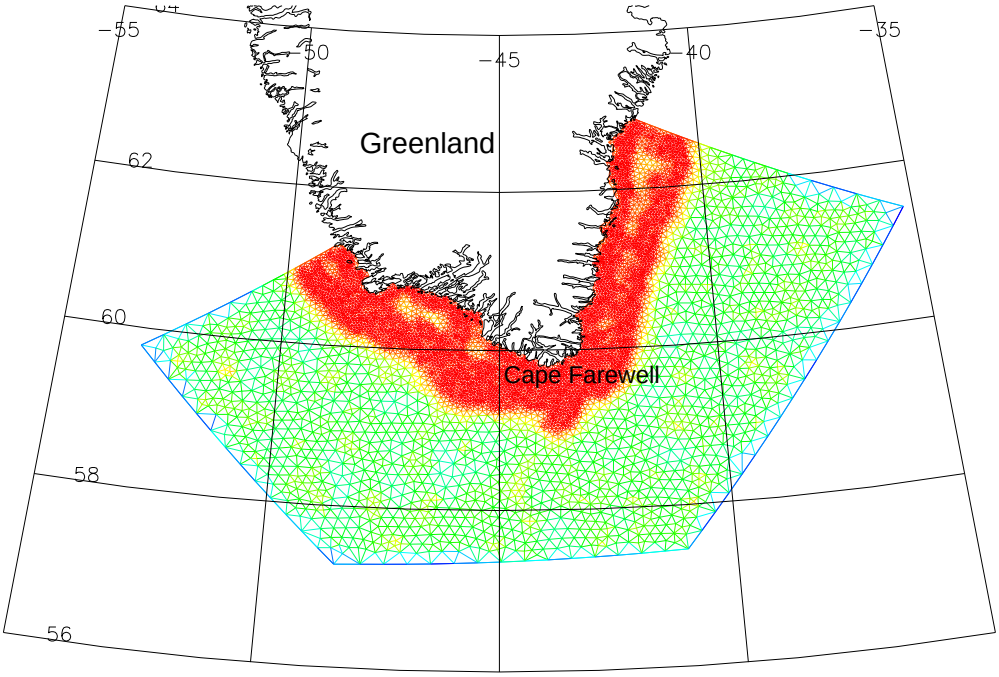

Figure 3. Computational mesh with 6349 nodes and 12476 elements.

equations. Currently the ice is considered as consisting of just one type, but the model can easily be extended to include several types, for example first year and multi year ice, with different properties.

The momentum equation includes the Coriolis force, a gravity force due to the tilt of the sea surface, the wind drag and sea surface current drag, and a force due to the divergence of the internal ice stress. The thickness and concentration fields evolve in time according to advection-diffusion equations.

The sea ice model includes the following features:

- Feasibility to choose between Cartesian and spherical coordinates.
- Discritisation by the finite element method.
- The cavitating fluid ice rheology [*Flato and Hibler*, 1992].
- Quadratic drag formulation of the air and water stresses.

The model is set up for a domain covering the area around Cape Farewell. The open boundary is splitted into three parts; two, which are normal to the coast and isobaths about 300 km up the east and west coasts, respectively, and an open boundary in deep water almost parallel to the coast about 250 km offshore. The inflow of water and sea ice takes place at the boundary normal to the east coast, and outflow is primarily at the boundary normal to the west coast, while the currents at the deep water boundary are small.

The computational mesh is shown in Fig. 3. It consists of 6349 nodes connected by 12476 elements. The generation of the mesh exploits the possibility with the finite element method to have a varying resolution, thus it has high resolution on the shelf and continental slope, where

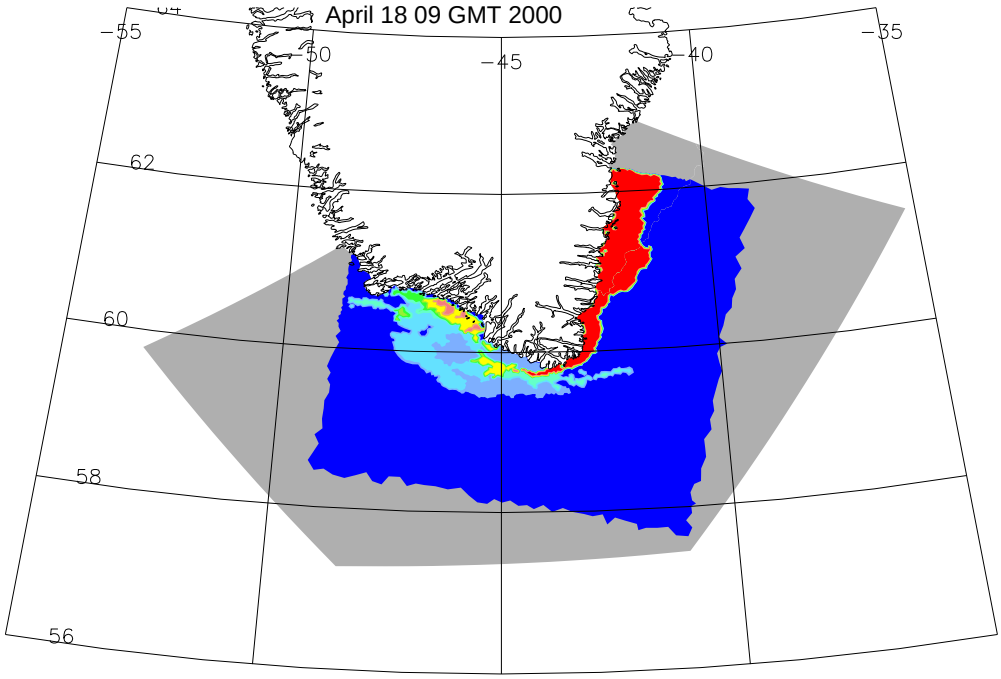

Figure 4. Sea ice map, 09 UTC 18 April 2000. Ice is shown with light blue (low concentration) to red (high concentration), blue color indicate open water, and gray indicate areas with no observations.

most of the ocean dynamics take place and where the ice is usually found. The colorscale indicate the resolution being from 2 km up to 23 km.

2.3 Sea ice observations

The ice observations are primarily made by the Radarsat satellite. These observations are made approximately once a day, with varying degree of coverage of about 50% to almost 100% of the model domain. The observations are received in real time at DMI. The analysis transforming a satellite image to a useful map of the sea ice cover are performed manually by special trained staff.

Figure 4 shows the analysed field at 09 UTC 18 April 2000. The extend of the Radarsat image is clearly seen, covering 52% of the model domain. Off the east coast of Greenland a high concentration of 0.9 is found and the ice edge is sharp. Off the west coast the concentration is much lower, having values of 0.1-0.4, and the ice fields consist of fields of different concentrations.

Figure 5 shows the coverage of analyzed ice fields through the ice season December 1999 to June 2000. Since the observations only cover a part of the model domain, the ice analyses do so too. Occasionally, the analyses are based on observations made at different time. This information is lost when the analyzed fields are transformed to gridded data, which just have a single time stamp. This is an error source with a negative influence on the validation of the numerical simulations, and these fields are therefore not included in the validation in section 4. Though, most of the paper versions of the ice maps contain the date information, and it has therefore been possible manually to remove old data from many of the analysed ice fields. These reduced ice fields are therefore representing a single dataset and are used in the validation equivalent to the true single dataset ice fields.

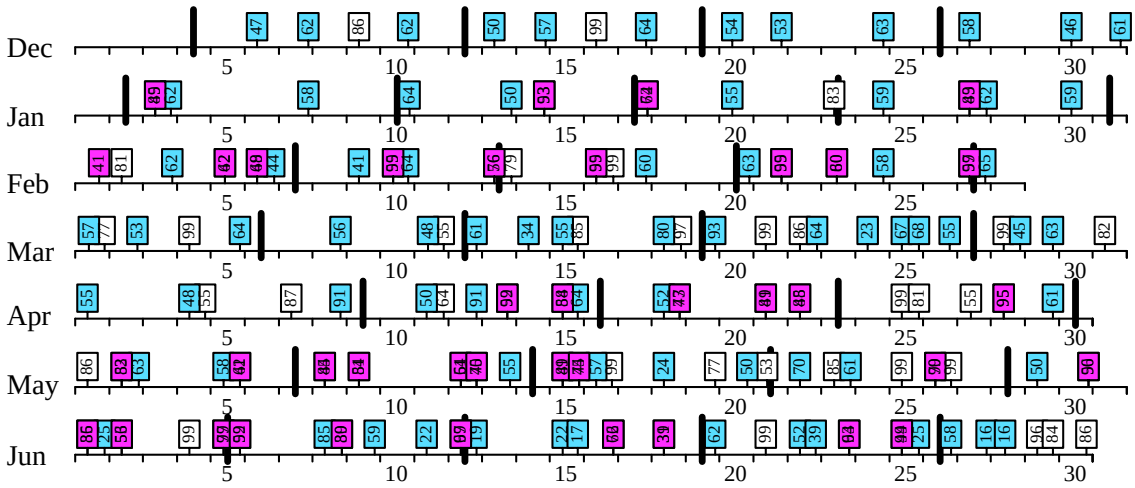

Figure 5. Produced ice maps December 1999 to June 2000. Maps based on a single dataset are shown by blue boxes, maps reduced to be based on a single dataset are shown by red boxes, while maps based on observations made at different time is shown by open boxes. The ratio of the area of the model domain covered by the map is given in percentage. The vertical solid lines indicate full coverage weekly ice maps.

Once a week a full coverage ice map is produced based on all available sources of information. These maps are assembled using data on different types and are not expected to be used in the daily forecast procedure. Though, due to their full coverage they are usefull as initial field for the very first forecast and if the continuity in the forecast procedure breaks, for example if the time interval between two succesive observations is larger than the forecast length.

2.4 Wind forcing

The model is forced by 10 m wind fields from the HIgh Resolution Limited Area Model (HIRLAM) run operationally at the Danish Meteorological Institute [*Sass et al.*, 1999]. The HIRLAM system consists of several nested models. The wind fields are extracted from the two models named "DMI-HIRLAM-G" and "DMI-HIRLAM-N" covering Greenland. DMI-HIRLAM-G is the coarser model with a resolution of 0.45° and a forecast length of 60 hours, while the inner model DMI-HIRLAM-N has a resolution of 0.15° and a forecast length of 36 hours.

2.5 Ocean forcing

The sea surface current and elevation used for the ocean forcing are calculated by the linear harmonic model, Fundy [*Lynch and Werner*, 1987; *Greenberg et al.*, 1998]. It is a diagnostic model where the time dependence is based on the assumption that the dependent variables are harmonic oscillating. Here is used zero frequency giving the steady-state solution.

The model is set up for a larger domain (see Appendix A) to remove boundary effect from the area of interest. The calculation is performed for a domain extending from 71°N at the east coast to 70°N at the west coast and down to 53.4°N at the open boundary in the Atlantic Ocean. The baroclinic part of the calculation is based on a rather arbitrary density field with Arctic water, i.e. water with a temperature of -1.5°C and a salinity of 33.3 psu on the shelf defined by the area

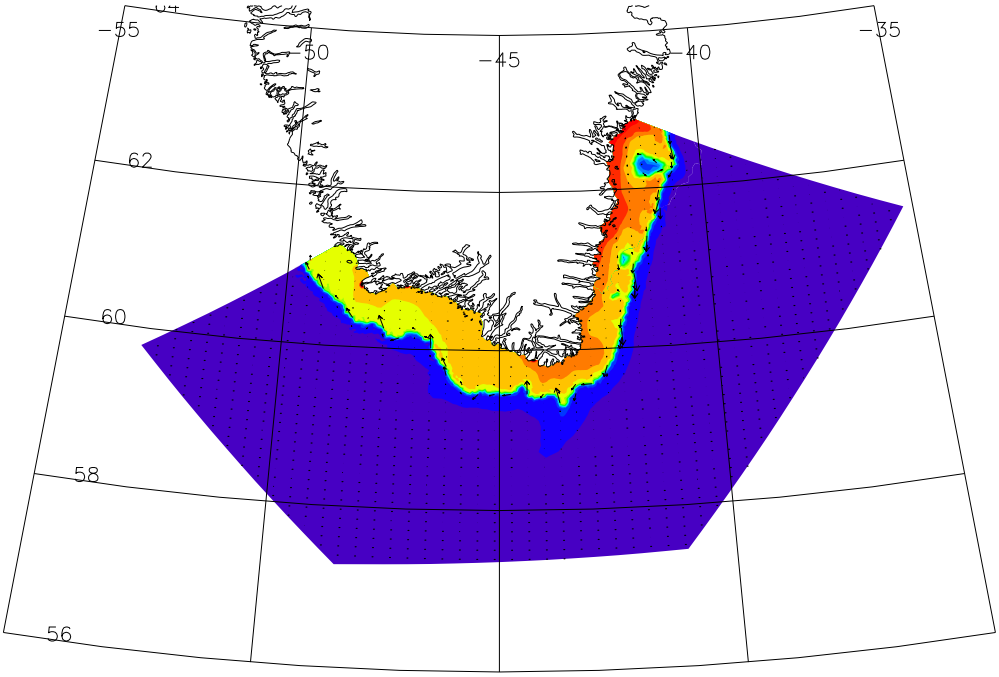

Figure 6. Sea surface current and elevation used for ocean forcing.

having a depth less than 570 m, and Atlantic water of 4°C and 35 psu elsewhere. The reason for this is mainly the lack of useful data and is a topic for further development.

The resulting elevation and surface velocity field (see Fig. 6) show a sharp elevation gradient and a strong current closely following the shelf break and the corresponding density front. Further off-shore the currents are very weak.

2.6 Example of forecast cycle

Figure 7 shows an example of two cycles of the forecast system. The observed field at 11 April is used as initial fields for a model simulation. At 13 April new observations are available, and the model is reinitialized. The observations do only cover the eastern part of the area, and the forecast from 11 April is used to fill out the missing values, and a new simulation is performed. At 15 April new observations are available, a new reinitialization is made, and so forth.

It shall be mentioned that the simulations shown here are from a period with relatively calm weather conditions and only small development in the ice cover is seen.

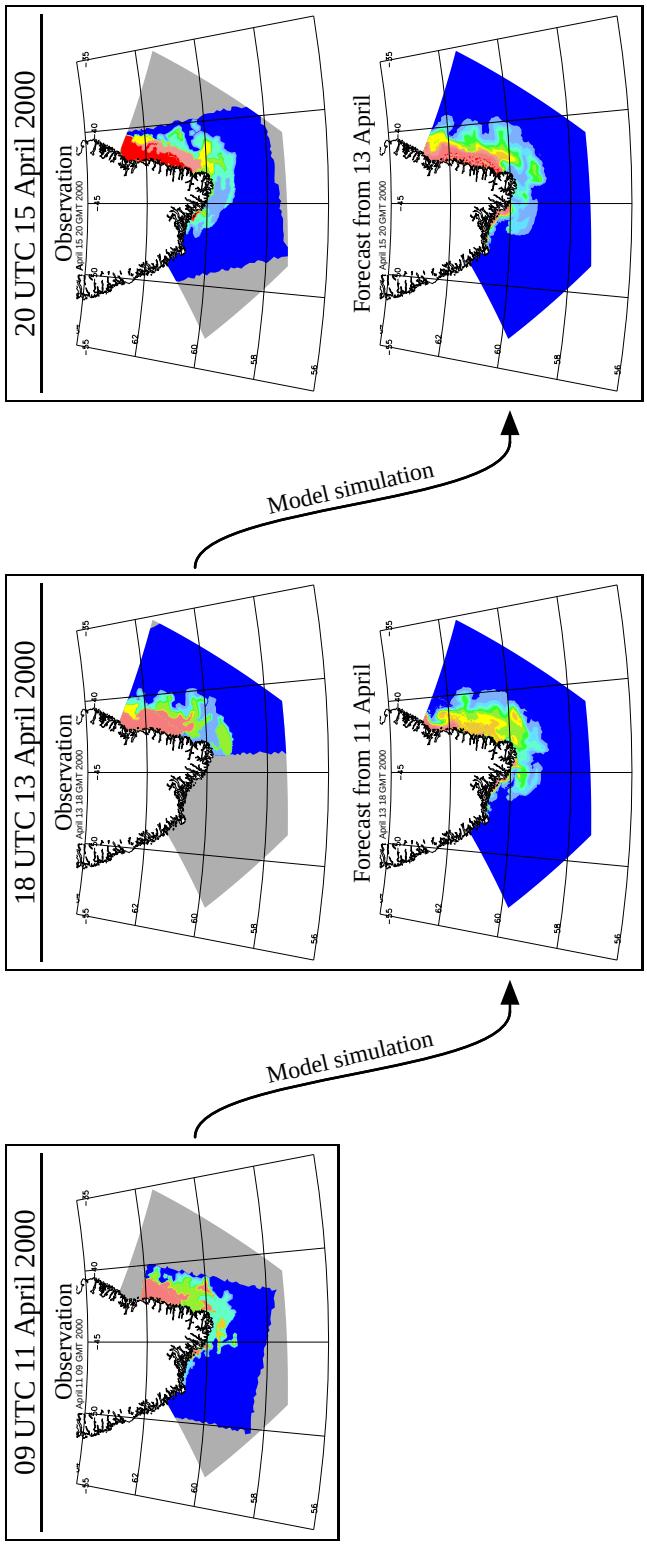

Figure 7. Two cycles of the system in the period 11-15 April 2000.

3 Numerical sea ice model

The numerical sea ice model is based on the assumption that the sea ice is a continuum with a velocity field $\vec{v}$, a thickness field h, and a concentration field A. The thickness is the area mean thickness, and the actual ice thickness is equal to h/A for $A \neq 0$. Currently the ice is considered as consisting of just one type, but the model can easily be extended to include several types, for example first year and multi year ice, each having a thickness and concentration.

The momentum equation includes the Coriolis force, a gravity force due to the tilt of the sea surface $\nabla\zeta$, the wind drag $\vec{\tau}_a$ on the ice, the surface current drag $\vec{\tau}_w$ on the ice, and a force $\vec{F}$ due to the divergence of the internal ice stress

$$\rho h\frac{\partial\vec{v}}{\partial t}+\rho h\vec{f}\times\vec{v}=-g\rho h\nabla\zeta+\vec{\tau}_a+\vec{\tau}_w+\vec{F} \tag{1}$$

where $\vec{f}$ is the Coriolis parameter written as a vector pointing upward and ρ is the density of sea ice.

The wind and ocean current stresses are calculated using the quadratic formulations

$$\vec{\tau}_a = AC_{ai}\rho_a\left|\vec{v}_a-\vec{v}\right|\left(\vec{v}_a-\vec{v}\right) \tag{2}$$

$$\vec{\tau}_w = AC_{wi}\rho_w\left|\vec{v}_w-\vec{v}\right|\left(\vec{v}_w-\vec{v}\right) \tag{3}$$

where C_{ai} and C_{wi} are dimensionless air-ice and water-ice drag coefficients, ρ_a and ρ_w are the air and water densities, and $\vec{v}_a$ and $\vec{v}_w$ are the wind and surface current velocities.

The internal ice stress is based on the cavitating fluid rheology [*Flato and Hibler*, 1992]. This rheology assumes that there is no shear stress, and no internal stress in the case of divergence, but there is resistance to compression, calculated as a pressure gradient ∇P. The pressure P is usually called the ice strength and depends on the thickness and concentration as

$$P = P^* he^{-C(1-A)} \tag{4}$$

where P^* and C are empirical constants.

The thickness and concentration fields evolve in time according to the advection-diffusion equations

$$\frac{\partial h}{\partial t} = -\nabla\cdot(\vec{v}h)+\nabla\cdot(D\nabla h) \tag{5}$$

$$\frac{\partial A}{\partial t} = -\nabla\cdot(\vec{v}A)+\nabla\cdot(D\nabla A) \tag{6}$$

where D is a diffusion-coefficient. The diffusion is necessary to keep the solution smooth and stable. Introducing a characteristic velocity scale V and a length scale Δl for the mesh, the ratio of the advection to the diffusion define the mesh Péclet number

$$Pe = \frac{V\Delta l}{D} \tag{7}$$

The model is run with a uniform mesh Péclet number throughout the domain and eq. 7 is used to calculate the diffusion coefficient for each element. V is the mean speed in the element, and Δl is

Variable	Symbol	Unit	Value
Density of ice	ρ	kg m^{-3}	910.0
Density of air	ρ_a	kg m^{-3}	1.3
Density of water	ρ_w	kg m^{-3}	1025.0
Air/ice drag coefficient	C_{ai}		$1.2 \cdot 10^{-4}$
Water/ice drag coefficient	C_{wi}		$0.5 \cdot 10^{-3}$
Ice strength parameter	P^*	N m^{-2}	$5.0 \cdot 10^3$
Ice strength parameter	C		20.0
Mesh Péclet number	Pe		5.0

Table 1. Physical parameters and constants.

the side length of the element assuming it is an equilateral triangle. Thus, the diffusion coefficient varies dependent upon the velocity and the distance between the nodes. It is noted that a high mesh Péclet number gives little diffusion and vice versa.

To make the model suitable for large domains, the feasibility of using latitude/longitude coordinates is included. This is done similar to *Greenberg et al.* [1998] by the transformation to curvilinear coordinates

$$\begin{aligned} dx &= R\cos(\phi)d\lambda \\ dy &= Rd\phi \end{aligned} \tag{8}$$

where λ and ϕ denote the longitude and latitude, respectively, and R is the radius of the earth.

4 Validation

4.1 Set-up

The system is validated in hindcast mode for the ice season December 1999 to June 2000, with the sea ice model set up as described in Section 2. The climatological ocean fields shown in Fig. 6 are used for the ocean forcing, and three-hourly wind fields from DMI-HIRLAM-G are used for the wind forcing.

The aim is to produce forecasts of about 3 days. A much longer simulation period of 10 days is nevertheless applied in this validation study in order to investigate the limit of the forecast system. Each simulation thus span several observations used for the validation.

The first simulation is initialized by the weekly mean ice map at December 4. This is the only weekly mean ice map used, and the proceeding simulations are all initialized at the time of available observations by combining the new observations with the preceding simulation. It is noted that only the ice concentration is observed. The thickness and velocity fields are reinitialized as follows. Where the concentration is zero, there is no ice, and the thickness and velocity is set to zero too. In case of ice, i.e. if the concentration is larger than zero, the thickness is set such that the actual ice thickness is 1 m, and the velocity is set to a geostrophic velocity according to the first 3 terms of Eq. 1.

4.2 Error estimates

The simulations are validated against the existing ice maps which is based on observations of ice concentration. The observations available are thus the ice concentration field at some given times, and the validation is performed for the simulated concentration at the observation times. The error is defined as the difference of ice concentration calculated with the sea ice model, A, and the observed concentration, A_{obs}. Since the observations cover only a part of the model domain, the comparisons are performed for these parts only. The error estimates are calculated as area mean values. The area mean is defined by

$$\langle A \rangle = \frac{\int_S A da}{\int_S da} \tag{9}$$

where the surface integration is performed on the area S of the domain that is covered by observation.

With the definition Eq. 9 the following statistical estimates can be calculated at a given time. The variance

$$\sigma^2(A) = \langle A^2 \rangle - \langle A \rangle^2 \tag{10}$$

The covariance

$$\sigma^2(A, A_{obs}) = \langle A \cdot A_{obs} \rangle - \langle A \rangle \cdot \langle A_{obs} \rangle \tag{11}$$

The correlation coefficient

$$\rho(A, A_{obs}) = \frac{\sigma^2(A, A_{obs})}{\sigma(A) \cdot \sigma(A_{obs})} \tag{12}$$

where the standard deviation is $\sigma(A) = \sqrt{\sigma^2(A)}$.
The root mean square error

$$\text{rms} = \sqrt{\langle (A - A_{obs})^2 \rangle} \tag{13}$$

4.3 Ice season December 1999 to June 2000

Figures 8 and 9 shows rms and $\rho(A, A_{obs})$ for the ice season from December 1999 to June 2000. The different simulations seem to have similar error statistics. From the simulation start to the first available observation after 30-50 hours the rms error is increased to about 0.1. Thereafter the rms error increases more slowly to a value between 0.1 and 0.25 after 240 hours. The correlation coefficient show a similar shape, though decreasing while the rms error is increasing.

There is a small seasonal trend, the forecast being slightly better in the first months than in the end of the period. This is probably because the sea ice model do not include thermodynamics and mechanical processes such as wave interaction. Thus, the ice removal and melting which is higher in the late spring than in the winter months is not included in the model. Neither is freezing, but this do not have the same influence in the model result since the main source of ice is the advection of ice to the area rather than localized freezing. Therefore, the error sources are smaller in the beginning of the ice season than in the end.

As mentioned, the correlation coefficient has a sharp decrease and the rms error increases in the first 30-50 hours for subsequently to level out, indicating that longer forecasts up to 10 days

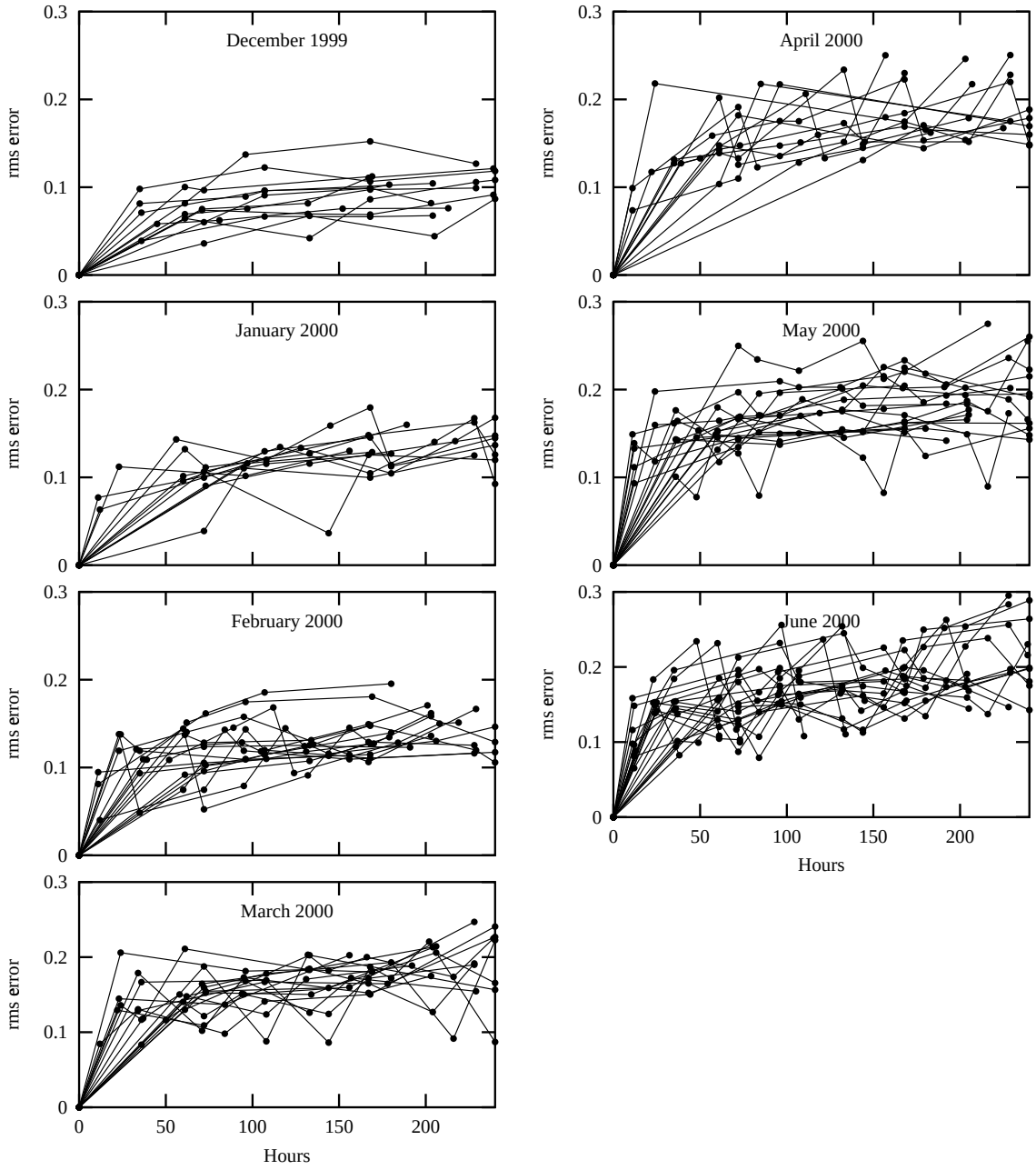

Figure 8. rms error of the ice concentration field.

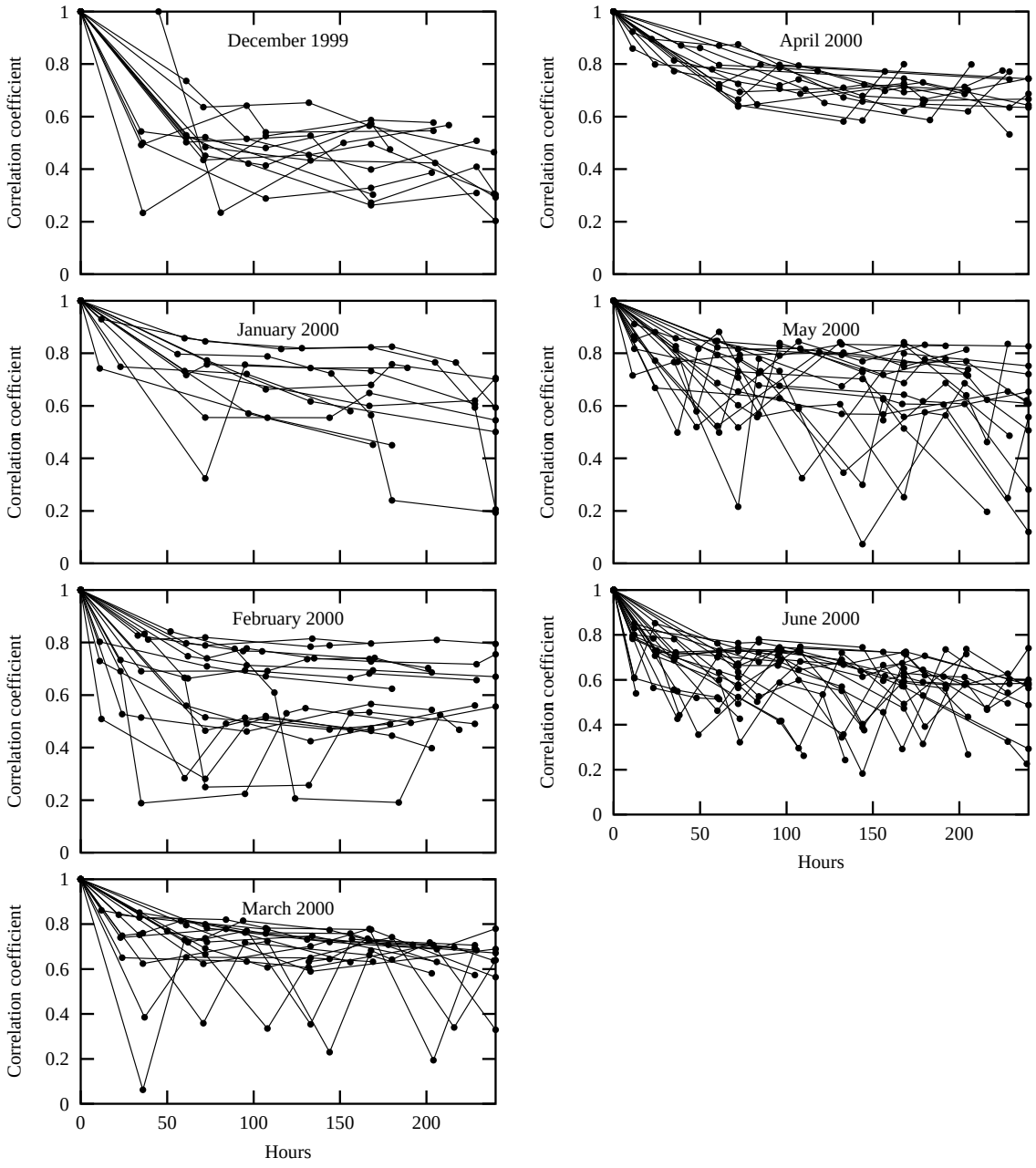

Figure 9. Correlation coefficient of the simulated and observed ice concentration field.

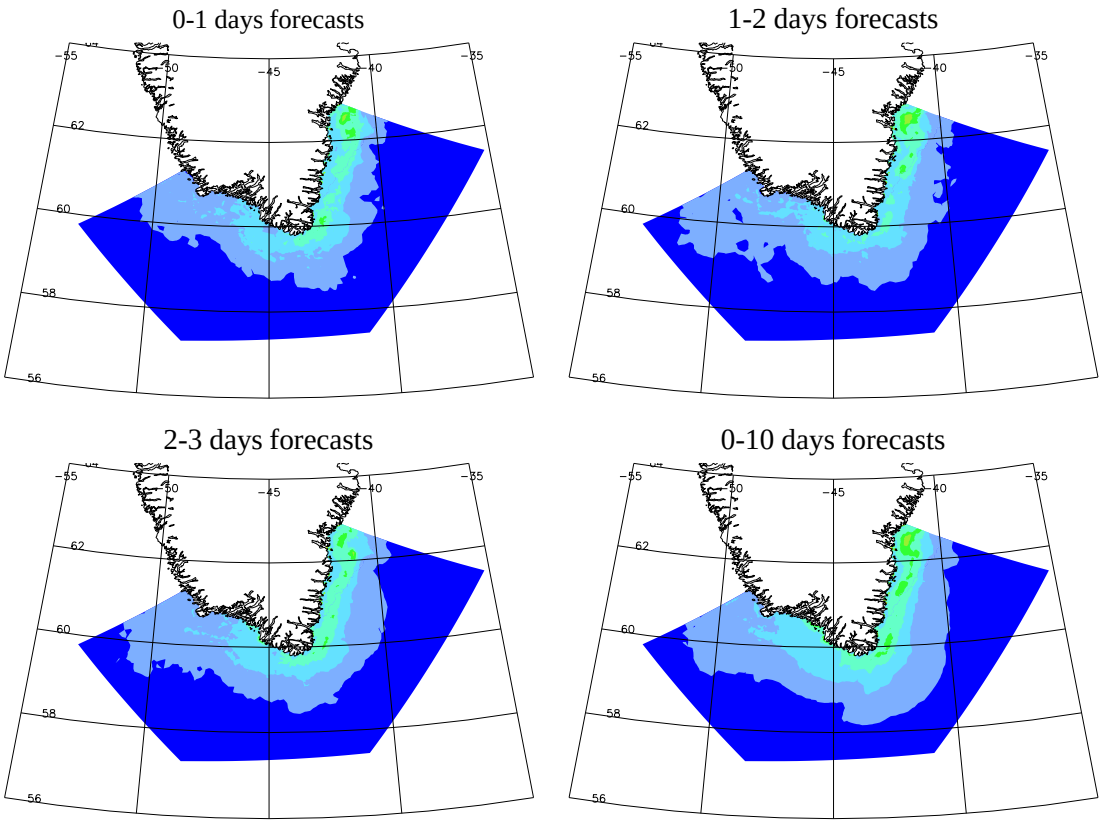

Figure 10. Absolute value of error. Averaged for 0-1, 1-2, 2-3, and 0-10 days.

might be feasible. Though, one should remember that the simulations reported here are hindcasts, and the maximum forecast length is limited not only by the errors in the sea ice model, but also by the atmospheric forecast length. The HIRLAM forecasts is 60 hours, while ECMWF do up to 7 days.

The spatial variation of the error is shown in Fig. 10 by mapping the absolute value of the error. The error fields are collected from all simulations and averaged in time to give a mean error field for 0-1, 1-2, 2-3 days and the 0-10 days average. The largest errors is found off the east coast of Greenland where the largest ice concentration also is found. This has probably to do with the pure numerical problem of the advection scheme smoothing the fields. Off the west coast errors of 0.1-0.2 is found for the ice concentration. A small increase of the values with time is found, as expected from the discussion above, but the pattern of the error is nearly unchanged.

4.4 Examples of simulations

Two simulations from the validation are presented here as examples. Simulated and observed ice concentration fields from the simulations started at 17 February and 13 April 2000 are shown in Figs. 11 and 12.

In the simulation starting at 17 February (Figs. 11) the ice is only present along the east coast initially in a narrow band close the coast. After 3 days the ice is moved slightly further south, and an offshoot has formed at about 62°N. This is also found in the simulation, although the

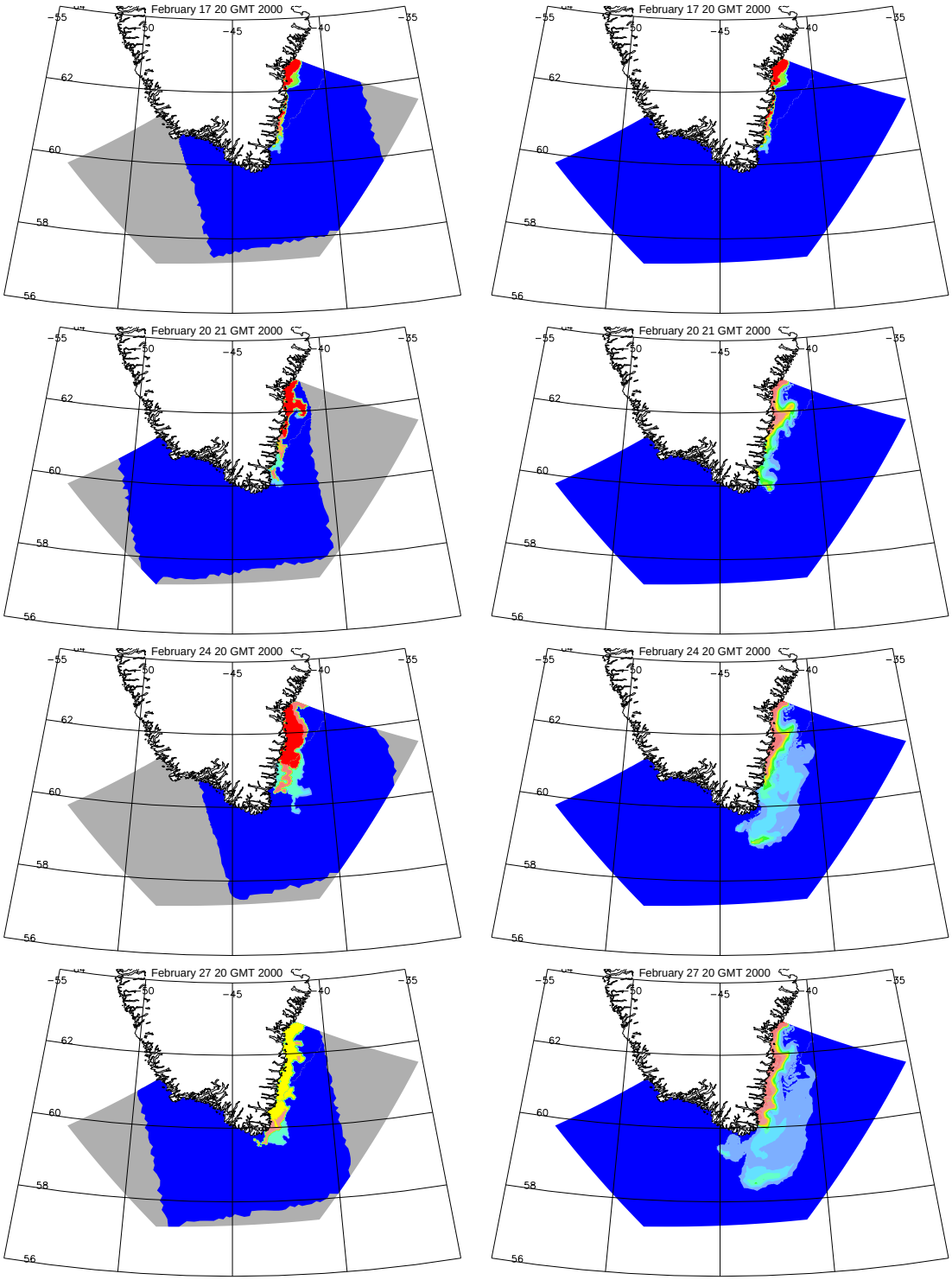

Figure 11. Ice concentration field for simulation started at 20 UTC 17 February 2000 (right column), and observations (left column).

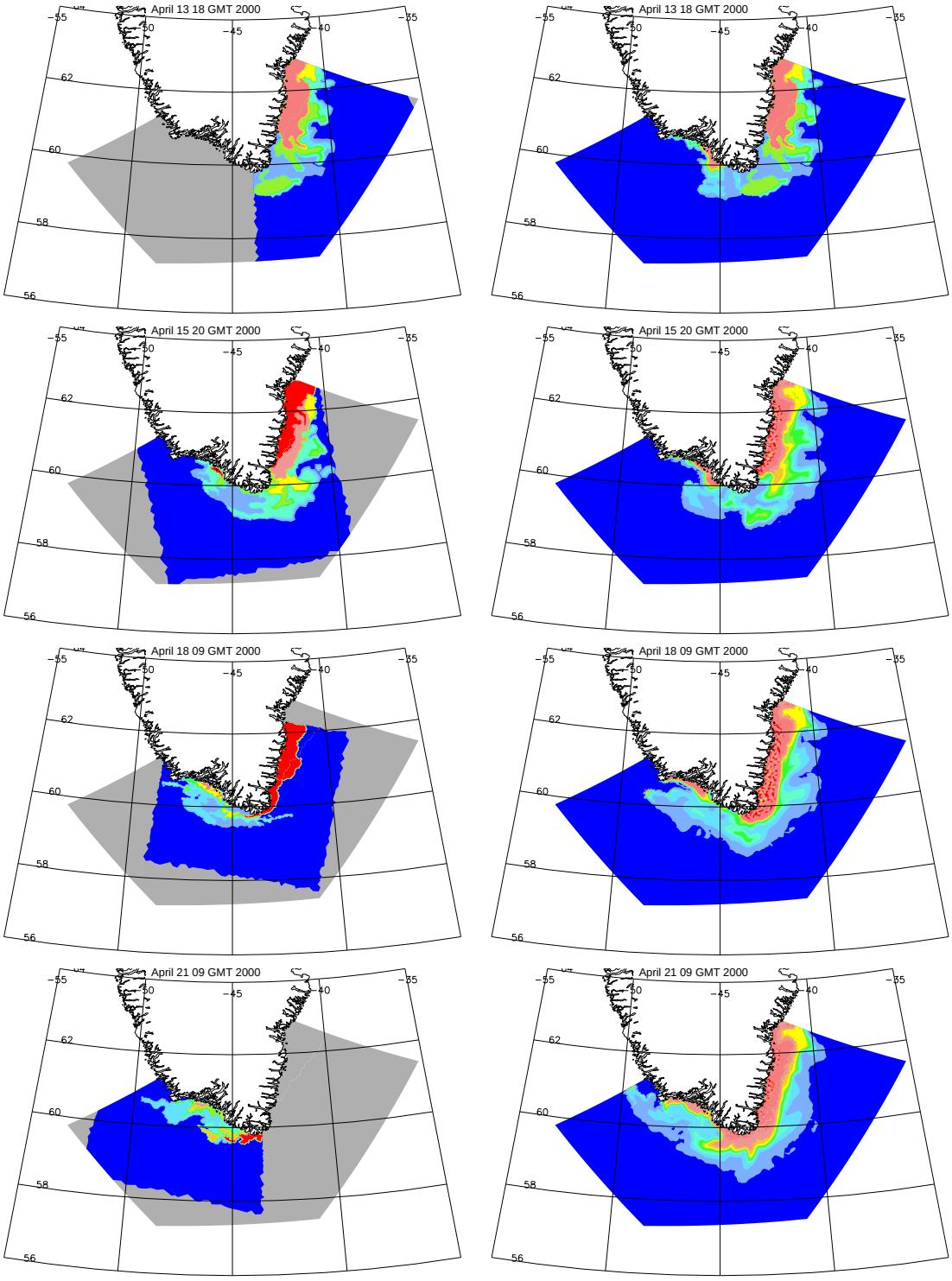

Figure 12. Ice concentration field for simulation started at 18 UTC 13 April 2000 (right column), and observations (left column).

offshoot has a slightly different form. Interestingly, the offshoot seems to be connected with a concavity at 63°-62°N which is seen in many of the simulations. This concavity is also seen in the bottom bathymetry influencing the ocean current and surface elevation by topographic steering and thereby influencing the ice cover. After 7 days the ice cover has broadened probably due to westerly winds and a increased inflow of ice. The model does not include the possibility of changed boundary conditions, and the information of these conditions is not available, but the model do respond to the wind. Therefore the ice cover is broadened, but the ice concentration is not simulated as high as observed. After 10 days the ice cover is observed to have narrowed and to have reached Cape Farewell. In the simulation the relatively large area with low concentration has no possibility to disappear, but disregarding this low concentration ice cover the simulation seems to agree much better with reality, even in a 10 days simulation.

In the other simulation[1] starting at 13 April (Figs. 12) the ice cover is more developed with high concentration of ice in a broad band along the east coast, and about 200 km up the west coast at lower concentration. After the first 2 days only small changes have happened. The area at the east coast with high concentration is extended slightly further south as is also seen within the model result. The model also captures the features with two areas of high concentration, one large area all along the east coast and a smaller area at the west coast, and in between lower concentration at Cape Farewell. After 4.5 days all the low concentration ice east of Greenland has disappeared, leaving the approximately 50 km wide band with high concentration and a sharp ice edge. The high concentration ice field has been pulled around Cape Farewell almost connecting the small area at the west coast with high concentration. While the area of low concentration east of Cape Farewell has totally disappeared, the area of low concentration west of Cape Farewell is almost unchanged. The simulation compare well west of Cape Farewell, and the high concentration on the east coast is also pulled, to some extend, to Cape Farewell. Though, the low concentration ice field is kept in the model. The reason is, as mentioned above, that there is no possibilities to remove the ice in the model. After 7.5 days the observation covers west of Cape Farewell only. At this date the simulation compares well, except for an extended area of concentration less than 0.1.

5 Conclusion

A sea ice forecasting system is set up for the Cape Farewell area, and validated for the ice season December 1999 to June 2000. The system is intended to be an extension of the present ice service at DMI. The product is the forecasts of the ice cover on a time scale of a few days. The system is build upon the nowcasting currently being performed at DMI, such that the observed ice fields is used for reinitialization of the forecast system.

The core of the system is a finite element dynamic sea ice model. The model is based on the traditional continuum assumptions. It includes transport equations for the ice concentration and thickness, and a momentum equation for the velocity, and is forced by the atmosphere and ocean. The wind fields are obtained from the operational atmospheric model at DMI, and the sea surface current and elevation are calculated by using a diagnostic ocean model. The ice model includes a simple ice rheology. This seems to be suitable for the Cape Farewell area where most of the ice undertake free drift, and the ice stress is just necessary in case of on-shore wind. Due to the simplicity of the ice rheology the computational speed is high.

The system is validated in hindcast mode for the ice season from December 1999 to June 2000.

[1] This simulation actually span over the example of an ice field shown in Fig. 4 and is the second simulation in the example of the forecast cycle shown in Fig. 7.

The error is found to have a steep increase in the first 30-50 hours for subsequently to level out. The largest errors are found along the east coast where also the highest concentrations are observed. The model is found to smooth the ice field and to spread the ice in a relatively large area. These large areas with low ice concentration are only occasionally found in reality, though now and then the ice is reported to be spread over a large area over night, for example in stormy weather. The overall consideration is that the general pattern of ice drift is simulated with reasonable results, and the forecasts should be of value for ship routing and other users. Furthermore the forecasts should be of value for the present ice service at DMI in the analysis of the ice observations.

The main emphasis of further development of the system is suggested to go into the ice model, but also the ice-ocean interaction is suggested to be considered for further investigation. The primary suggestion for further development is to implement thermodynamics, maybe just a simple scheme, and/or a parameterization of ice removal by wave interaction. This will influence the areas with low concentration. In reality, as the concentration is lowered, the effect of thermodynamical processes as well as mechanical processes, such as wave interaction, is increased. Thus as the ice is spread, the concentration is lowered, and the ice is quickly breaked down and melted. With these processes implemented in the ice model, the results are expected to improve, especially in the late spring where melting is becoming more and more important.

Another topic for further development is the forcing of the model. The atmospheric forcing is extracted from HIRLAM, the operational atmospheric model at DMI. The wind fields are expected to be the best possible for this area, even though the observations are sparse, and it is probably not worth to put too much effort into any investigations of the atmospheric fields. The ocean forcing is calculated by a diagnostic model. The wind effect on the ocean is not taken into account, neither is the tides. This is an obvious topic for further development. The aim should be to have a three dimensional prognostic model running with a high vertical resolution near the surface. This way the wind effect on the sea surface will be included, the tides should be taken into account as well, and the time evolution of the ocean temperature will be of importance for the thermodynamical processes in the sea ice model. Though, it shall be noted that the computational time of a three dimensional prognostic ocean model does not at all compare to that of the ice model. The ice model forced by a steady state ocean is very quick, and can be executed even on a pc. The sea ice forecasting system is therefore most easily being improved by further development of the ice model, while including a prognostic model will be on a longer perspective.

A Waters around Greenland

The aim in this study is to establish the sea ice forecast system for the Cape Farewell area. On a longer perspective the forecasts should be produced for a larger domain. The mesh used for the ocean simulations is shown in Fig. 13. It covers the larger domain extending from 71°N at the east coast to 70°N at the west coast and down to 53.4°N at the open boundary in the Atlantic Ocean. The color indicate the resolution being about 2 km on the shelf and continental slope up to 57 km at the open boundaries at deep water in the North Atlantic. The Cape Farewell mesh shown in Fig. 3 actually is a part of this mesh with a higher resolution than the surrounding areas.

The difficulties with this larger domain are to get initial ice fields. The reason for concentrating on the Cape Farewell area is that this is currently the most important area with respect to ship traffic, but also that the Radarsat observations, and thereby the analysed ice fields cover this area only. If the forecasting system is to be applied to the larger area, other information has to be used for the initial condition. This could be the weekly maps which covers all around Greenland.

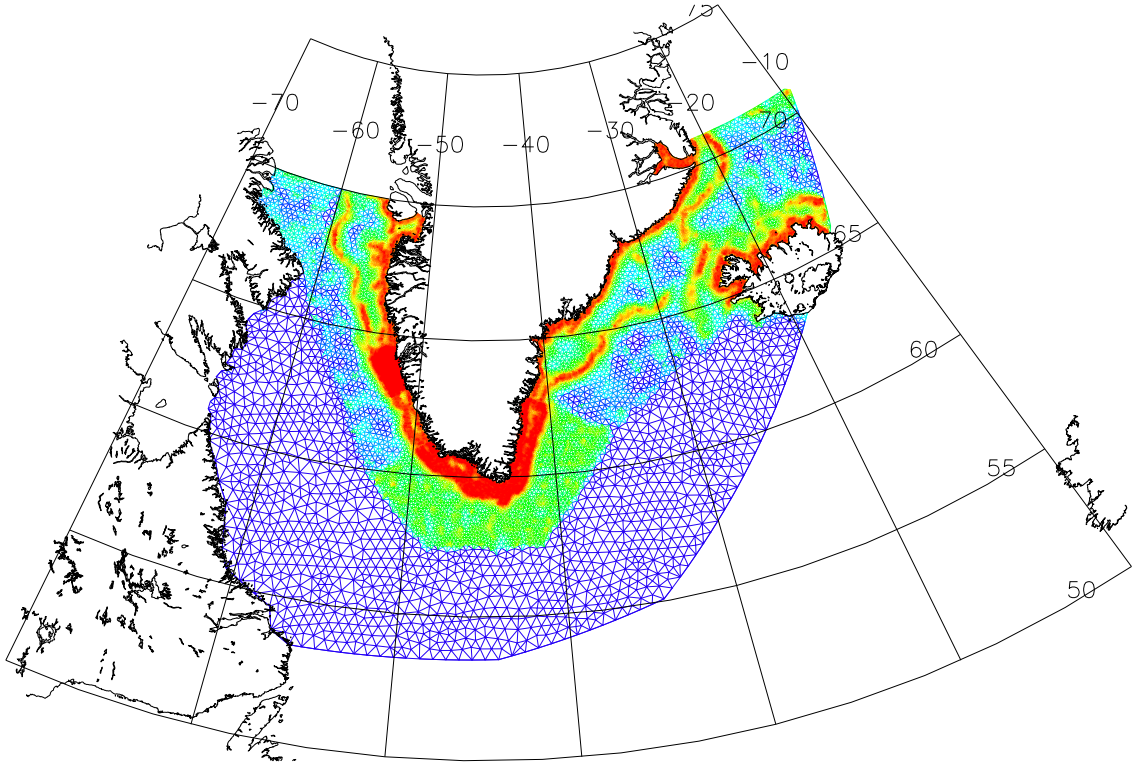

Figure 13. Computational mesh of the larger domain with 21230 nodes and 41417 elements.

References

Flato, G. M., and W. D. Hibler, III, Modeling pack ice as a cavitating fluid, *J. Phys. Oceanogr.*, *22*, 626–651, 1992.

Gill, R. S., Evaluation of the RADARSAT imagery for the operational mapping of sea ice around Greenland in 1997, *Scientific Report 98-5*, DMI, Copenhagen, Denmark, 1998.

Gill, R. S., and H. H. Valeur, Ice cover discrimination in the Greenland waters using first-order texture parameters of ERS SAR images, *Int. J. Remote Sensing*, *20*, 373–385, 1999.

Greenberg, D. A., F. E. Werner, and D. R. Lynch, A diagnostic finite-element ocean circulation model in sperical-polar coordinates, *J. Atmos. Ocean. Technol.*, *15*, 942–958, 1998.

Kliem, N., Numerical ocean and sea ice modelling: the area around Cape Farewell, Ph.D. thesis, Departement of Geophysics, NBIfAFG, University of Copenhagen, Copenhagen, Denmark, 1999.

Lynch, D. R., and F. E. Werner, Three-dimensional hydrodynamics on finite elements. part I: Linearized harmonic model, *Int. J. Numer. Methods Fluids*, *7*, 871–909, 1987.

Sass, B. H., N. W. Nielsen, J. U. Jørgensen, and B. Amstrup, The operational DMI-HIRLAM system, 2nd rev. ed., *Technical Report 99-21*, DMI, Copenhagen, Denmark, 1999.